

Pushing multiphoton resonant ionization of the argon atom to the low-intensity regimeXuan Yu,^{1,*} Na Wang,^{3,*} Jian-Ting Lei,^{1,2} Jian-Xiong Shao,^{1,†} Toru Morishita,⁴ Song-Feng Zhao,³ Bennaceur Najjari,² Xin-Wen Ma,^{2,5,‡} and Shao-Feng Zhang^{2,5,§}¹*School of Nuclear Science and Technology, Lanzhou University, Lanzhou 730000, China*²*Institute of Modern Physics, Chinese Academy of Sciences, Lanzhou 730000, China*³*Key Laboratory of Atomic and Molecular Physics and Functional Materials of Gansu Province, College of Physics and Electronic Engineering, Northwest Normal University, Lanzhou 730070, China*⁴*Institute for Advanced Science, The University of Electro-communications, 1-5-1 Chofu-ga-oka, Chofu-shi, Tokyo 182-8585, Japan*⁵*University of Chinese Academy of Sciences, Beijing 100049, China*

(Received 10 November 2021; revised 16 April 2022; accepted 28 July 2022; published 22 August 2022; corrected 30 August 2022)

Resonance-enhanced multiphoton ionization process of the argon atom by an 800-nm 30-fs linearly polarized laser field is investigated at intensities range from 1.1 to 4.55×10^{13} W/cm². At 4.55×10^{13} W/cm² intensity the experimental photoelectron energy spectrum is in a good agreement with the time-dependent Schrödinger equation (TDSE) calculation where the double structure originating from dressed $4p - 4d$ coupled transition is clearly identified. At lower intensity of 1.1×10^{13} W/cm², the resonant ionization process via the $4f$ state is observed, however, the expected peak (jet) at 90° in the photoelectron angular distribution from the zeroth order above threshold ionization, has vanished completely. Such behavior is attributed to the destructive interference phenomenon in the coherent contributions of different partial waves of the photoelectron, namely, ϵd and ϵg states, and has been confirmed in our TDSE calculations.

DOI: [10.1103/PhysRevA.106.023114](https://doi.org/10.1103/PhysRevA.106.023114)**I. INTRODUCTION**

Interaction between intense laser and matter have triggered tremendous studies that could not have been performed before the advent of short pulse intense lasers. Among these studies, the above threshold ionization (ATI), the high-order-harmonic generation, the sequential and the nonsequential ionization, to name a few, represent the most commonly studied processes in strong-field experiments (e.g., see reviews [1,2]). In the ATI process the number of absorbed photons by the atom can exceed that required to overcome the ionization potential. Therefore, a sequence of equally separated peaks by the photon energy are observed in the photoelectron spectrum (PES), and the excess number (S) of absorbed photons is called the ATI order. By consecutively adjusting the wavelength or intensity of the laser to measure the photoelectron energy and momentum distributions, various experiments have, thus, been performed during the past few decades (for instance, see Refs. [3–12]) to explore the embedded laws of its underlying physics. In these studies, the photoelectron angular distribution (PAD) has been a very well suited tool which can provide detailed information on quantum dynamics of atomic and molecular systems. As an important result, for low-order ATI the PAD pattern exhibits a jetlike structure where the number of minima can be directly associated

with the dominant angular momentum of the photoelectron [3,13–15].

From theoretical part, different studies have been developed for a better understanding and prediction of the PAD. It has been shown in Ref. [16] that the origin of the jetlike structure arises from the inherent properties of the ATI process, which is represented by the generalized Bessel function [17] but not from the angular momentum of either the initial or the excited states of the atom. For instance, according to the work of Bai *et al.* [18] the jetlike structure of PAD is due to the maxima of generalized phased Bessel functions but cannot be taken as an indication of the quantum number of the photoelectron angular momentum state. Later an empirical rule was proposed in Ref. [19] to predict the dominant angular momentum near threshold photoelectron. It is pointed out in Ref. [19] that, close to the threshold, the number of jets in the PAD depends strongly on the number of absorbed photons and unless the latter is increased due to the change in the laser intensity to populate the next ionization channel, the number of jets will remain unchanged. At this turning point a different minimum number of absorbed photons is required according to the new laser intensity. By comparing the numerical solution of time-dependent Schrödinger equation (TDSE) and the calculation of classical-trajectory Monte Carlo with tunneling, Arbó and co-workers [13,20] showed that the PAD mainly results from the interference of different pathways of the ionized electron and derived a semiclassical expression to predict the dominant angular momentum near the threshold.

Besides, in the PES discrete narrow energy peaks resulting from Freeman resonance [21] are observed in the ATI process. This is because when the energy difference between a

*These two authors contributed equally.

†shaojx@lzu.edu.cn

‡x.ma@impcas.ac.cn

§zhangshf@impcas.ac.cn

Rydberg state with an AC-Stark shift and the ground state equals to an integer number times the photon energy, the electron is likely to be first excited to a resonant Rydberg state, then consecutively removed to the continuum by absorption of extra photons. Because of the large ionization rate of such a resonant process, it is usually called resonance-enhanced multiphoton ionization (REMPI). In the case of nonresonant ionization, the ionization threshold of the atom is shifted in the intense laser field due to the influence of the ponderomotive potential. Since the latter depends linearly on the laser intensity [22] and shifts the positions of the nonresonant ionization peaks, it could be used to calibrate the laser intensity. However, the peak positions in PES of the resonant ionization process are independent of the laser intensity, which reflects the characteristic of the resonant ionization.

Resonant ionization process can unveil abundant dynamic information, such as AC-Stark splitting, the property of intermediate states, channel switching effect [8,23], interference of different quantum paths [24,25], and time delay of different resonant ionization channels [26,27]. Various resonant states [4,5,28] are reported in the intensity-resolved spectra of argon atom at comparably large intensities of $0.5\text{--}7 \times 10^{14}$ W/cm². However, to the best of our knowledge, for intensities below 3×10^{13} W/cm² (11-photon ionization process) the studies in this field remain scarce.

In this paper, photoelectron momentum and energy distributions of single ionization of an argon atom, in the linear-polarized laser pulses with a central wavelength of 800 nm and pulse duration of 30 fs, are measured at intensities of 1.1 up to 4.55×10^{13} W/cm² using reaction microscope. The paper is organized as follows, the next section describes the experimental setup, the discussion of the main results are presented in Sec. III. Then, Sec. IV, contains the summary of the main conclusions.

II. EXPERIMENTAL SETUP

In the experiment, linear-polarized laser pulses with a central wavelength of 800 nm and a full width at half maximum of 100 nm are used as the seed laser. After two stages of amplification the pulse duration of 30 fs can be achieved with a repetition frequency of 3 kHz and the maximum energy of each pulse can reach up to 5 mJ. The laser beam is then focused on the target zone of the reaction microscope by a convex lens whose focal length is 30 cm. The argon atomic target is prepared via the supersonic expansion which has a low-momentum spread at low temperature of a few Kelvins. Single-ionization events are selected by the three-fold coincident measurement among the recoil Ar⁺ ion, the photoelectron, and the laser pulse. The electric-field strength of time-of-flight (TOF) spectrometer is set to ~ 2 V/cm and the magnetic-field strength is about 4 G, which allow us to collect the electrons with the maximum transverse momentum up to 0.7 a.u. Detailed information about the laser system and reaction microscope can also be found in previous works of Refs. [29,30]. The laser intensity is determined from positions of the nonresonant ionization peaks according to Ref. [31]. Meanwhile, the pulse energies were also recorded throughout the whole experiment from which the laser intensities for the spectrum without clear nonresonant ionization peaks can also

be deduced. The uncertainty due to the calibration is estimated to be less than $\pm 5\%$. In our experiment the laser intensity is controlled by an adjustable attenuator in the beam line, and the intensities of $1.1\text{--}4.55 \times 10^{13}$ W/cm² can be obtained.

III. RESULTS AND DISCUSSIONS

Figure 1 shows the experimental results of the two-dimensional photoelectron momentum distributions of argon atom ionized by a linearly polarized (800-nm and 30-fs) laser field at different laser intensities of 1.1, 1.6, 2.0, and 4.55×10^{13} W/cm² as depicted in panels (a)–(d), respectively. The horizontal axis is the momentum component along the laser polarization and the vertical axis is the momentum component along the propagation direction of the laser. Radial fanlike structures in the form of jets from the nonresonant ionization process are depicted in all spectra except for Fig. 1(a), marked by the red dashed-dot circle. These radial fanlike structures are due to the interference between different pathways of the photoelectron [13,33]. The number of jets in these fanlike structures is different at different intensities of the laser field. For instance, six jets for a dominant angular momentum $l = 5$ are observed for 4.55×10^{13} W/cm² in Fig. 1(d), meanwhile, seven jets for a dominant angular momentum $l = 6$ are found when the intensity decreases to 2.0×10^{13} W/cm² and below as shown in Figs. 1(b) and 1(c).

The change in the number of jets of the radial fanlike structures indicates that at such intensity range there are two electron-emission channels, namely, 11-photon and 12-photon ionization channels where the atom absorbs, at least, 11 or 12 photons to release the photoelectron. Due to the conservation of the angular momentum the final electronic states, thus, have different parities for these two channels, resulting, respectively, in an odd or an even number of jets in the two-dimensional- (2D-) momentum distributions.

Furthermore, the 2D-momentum distribution shown in Fig. 1(d) exhibits sharp rings, originating from the REMPI involving different intermediate states, superposed on a radial fanlike structure. To assign these intermediate states the PES of Fig. 1(d) as an illustration is plotted in Fig. 2 where the horizontal axis is the photoelectron energy, and the vertical axis is the normalized yield. Meanwhile the TDSE calculation based on single active electron approximation (SAE) by the method in Ref. [34] with the atomic potential model from Ref. [35] is also presented in Fig. 2. In the calculations, the laser focal volume averaging is considered for a better comparison with the experimental data [34]. The spectrum shows that the intermediate states $ng(l = 4)$ with $n = 5\text{--}7$ as well as $np(l = 1)$ and $nd(l = 2)$ with $n = 4$ are clearly distinguished where n is the principal quantum number and l is the orbital angular momentum. It is noted that the peak structure at 1.6 eV cannot be unambiguously assigned to the lower resonant state below the $4d$ state, and the corresponding TDSE calculation shows that it results from the dressed transient $4p\text{--}4d$ states [28]. However, significant deviations are seen in the peak positions for the dressed $4p\text{--}4d$ coupled states, between our data and the calculation, despite that good agreement is achieved for the resonant ionization via intermediate ng states ($n=5\text{--}7$).

For instance, the TDSE results give the splitting of 0.17 eV in between $4p$ and $4d$ resonant ionization peaks whereas our

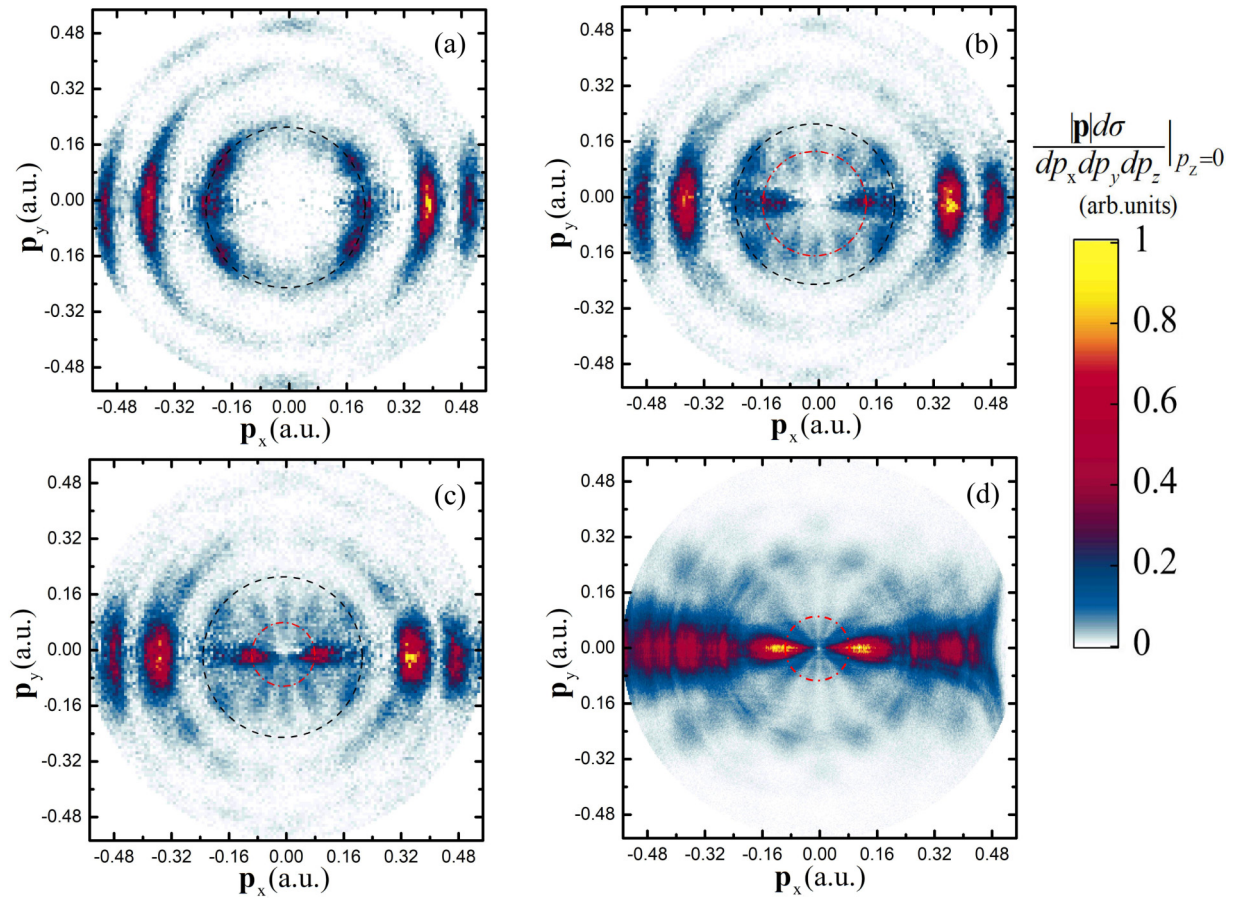


FIG. 1. Two-dimensional photoelectron momentum distributions of the argon atom in a linearly polarized (800 nm and 30 fs) laser field at intensities: (a) 1.10×10^{13} W/cm²; (b) 1.60×10^{13} W/cm²; (c) 2.00×10^{13} W/cm²; (d) 4.55×10^{13} W/cm². The horizontal axis P_x is the momentum component parallel to the laser polarization, and the vertical axis P_y is the momentum component along the propagation direction of the laser. The black-dashed ring line indicates the photoelectron with 0.225-a.u. momentum. Note that the abnormal strong node around $p_x \sim 0.5$ a.u. in (d) is due to the loss of kinetic information in the detector plane where the TOF of the emitted electron equals an integer of the electron cyclotron period in the magnetic field of the reaction microscope [32].

experimental data read at about 0.28 eV which is 63% larger than the prediction. According to Refs. [36,37], AC-Stark splitting is proportional to the Rabi frequency of $\langle a|r|b \rangle E$, where $\langle a|r|b \rangle$ is the transition matrix element between two coupled states, and E is the electric-field strength. Since the accuracy of our laser field intensity is less than $\pm 5\%$, it is, thus, safe to rule out possibility that the enhanced splitting is from higher laser field strength (E). Considering the fact that the $4p$ and $4d$ states are low-lying levels where the electron correlations and spin-orbit interaction should be stronger than those with higher principle quantum numbers ($n > 4$), the discrepancy could be attributed to the employed SAE model which neglects these effects in the calculations.

The PESs at intensities from 1.1×10^{13} to 2.4×10^{13} W/cm² are presented in Fig. 3 for a systematic comparison. One can see from these spectra that the position of the peak at ~ 0.7 eV remains the same regardless the laser intensity. Such a peak corresponds to the (10+1)-photon REMPI channel in which ten photons are required to populate the $4f$ state and then by absorption of an additional photon the electron is ejected to the continuum. In what follows we will keep a similar notation ($N+1$) photon for the specific REMPI process, where N stands for the number required photons for

resonant excitation to a transient Rydberg state whose energy is shifted due to the AC-Stark effect.

In the case of resonant ionization with the increase in the laser intensity or photon energy, the channel switching effect [23] modifies the number of required photons for the resonant population of given Rydberg states and determines the parity of involved resonant states of the REMPI process. In earlier studies [38], the angular momentum of these resonant states was attributed to the number of observed minima in the PAD. Later in Ref. [11], it was also shown that the PAD of the resonant ionization may also be directly related to the principal quantum number of the resonant states. As the laser field becomes stronger and close to the tunneling regime, it is reported that the patterns in the PAD with the same ATI order can involve two different intermediate states ($4f$ and $5g$) and have almost identical angular distributions [4].

Empirically, the number of minima between jets in the PAD equals $l \pm 1$ for an emission angle ranging between 0 and 180° in ($N+1$)-photon resonant ionization processes due to the angular momentum conservation with l being the orbital angular momentum of the intermediate Rydberg state. Consequently, it will present a minimum at 90° for even l , whereas a maximum is expected when l is odd. This empirical

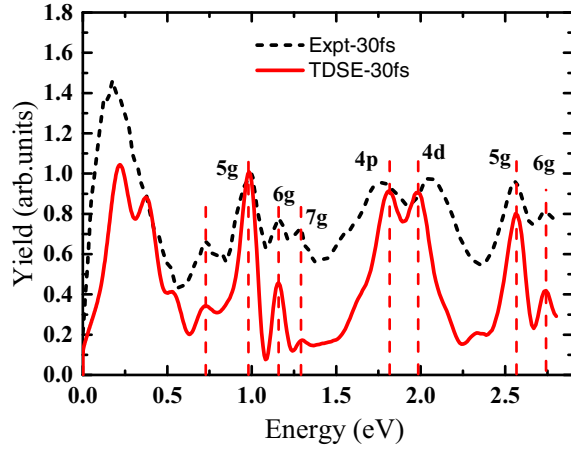


FIG. 2. Energy distribution of the photoelectron from the argon atom. (a) The black-dashed curve represents our experimental results at an intensity of 4.55×10^{13} W/cm² with 30-fs pulse duration for $|\theta| < 5^\circ$, θ is the angle between the direction of emitted electron and the laser polarization. The red-solid line is the corresponding TDSE calculation at $\theta = 0^\circ$ with the laser focal volume averaging. The experimental results are normalized to the 5g resonant ionization peak of TDSE calculation.

law has been widely used to explain the experimental results and even applies to high-order ATI processes [3,6,9–11,28]. However, as shown in Fig. 1(a) the 2D-momentum distributions and the corresponding angular distribution in Fig. 4(b) of (10+1)-photon resonant ionization via 4f state seems, at the first glance, to contradict the empirical law since no peak in the jet structure at 90° is observed as expected. The same feature is also reproduced by our TDSE calculation using the atomic potential of Muller and Kooiman [35] (Fig. 4). It should be noted that, in our TDSE calculation, the focal volume effect is not considered for two reasons which are as follows: (1) at such a low experimental intensity only those argon atoms exposed to the highest laser intensity can be

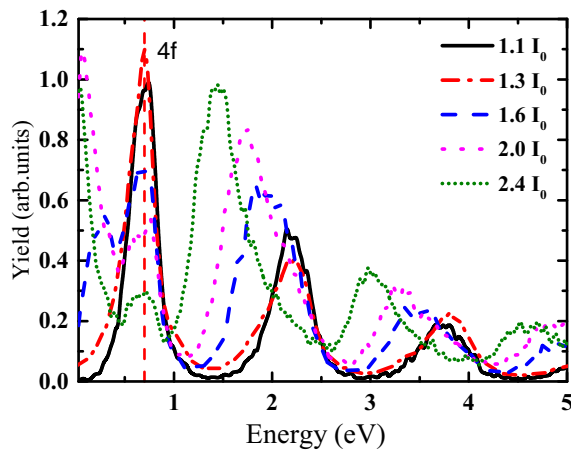


FIG. 3. Experimental results for the angle-integrated photoelectron spectra from the argon atom at various laser intensities lower than $2.4 \times I_0$ with $I_0 = 10^{13}$ W/cm². The black-dashed vertical line represents the peak position of 4f resonant ionization by absorption of the (10+1) photon.

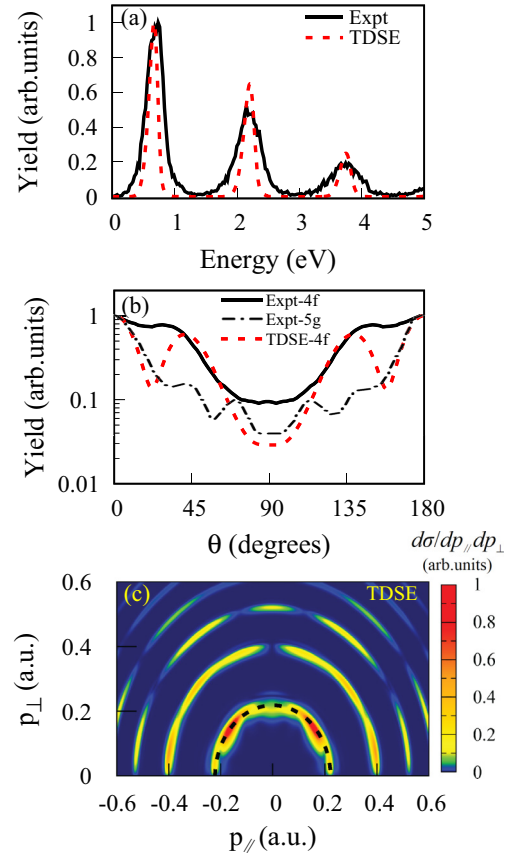


FIG. 4. Results of our TDSE calculation and our experimental data at an intensity of 1.1×10^{13} W/cm². (a) Photoelectron energy distribution; (b) photoelectron angular distribution for (10+1)-photon resonant ionization via the 4f state (the solid line), meanwhile photoelectron angular distribution for the (11+1)-photon resonant ionization via 5g (the dashed-dot line) from the present experimental data is also provided for comparison, θ is the polar angle of emitted electron with respect to the laser polarization; (c) TDSE results of the two-dimensional momentum distributions. Black-dashed half-ring indicates the (10+1)-photon resonant ionization via 4f state.

efficiently ionized and, (2) since the laser intensity is very close to 4f resonance intensity, the nonresonance ionization rate is practically negligible which can be confirmed by the present experimental data.

The absence of the lobe at 90° can be attributed to the destructive interference between ϵg ($l = 4$) and ϵd ($l = 2$) waves. From the TDSE calculation it is seen that for intensity of 1.1×10^{13} W/cm², starting from the 4f resonant state, the final angular momentum l of the photoelectron at the first resonant ionization peak equals to 0, 2 and 4, and their contributions are of 22.8%, 18.9%, and 54.7%, respectively. (Here the population to $l = 0$ continuum can be achieved through three photon processes where two photons are absorbed and a photon is emitted, see discussions in Ref. [28]). Indeed, the dominant contribution of the final state is from $l = 4$ which confirms the empirical predictions. However, the destructive interference between ϵg ($l = 4$) and ϵd ($l = 2$) waves completely washes out the lobe at 90° , meanwhile the ϵs wave ($l = 0$) practically has no contribution since it contributes evenly in all directions.

It should be noted that in the work of Ref. [4] it is reported that neither $4f$ nor $5g$ state exhibits a lobe structure at 90° and both PADs present almost identical patterns with five minima. The authors claim that the angular distributions are not associated with the quantum numbers of any particular resonant state. However, in their work ionization of argon was studied at laser intensities ranging from 2.0 to 8.0×10^{14} W/cm² which is one order of magnitude higher than our case. With such high intensities, different N-photon ionization channels arise [34] and the assignment of intermediate states, thus, becomes cumbersome and inaccurate. In Ref. [6] at lower intermediate laser intensities ranging from 0.8 to 2.0×10^{14} W/cm², a very strong jet structure at 90° with four minima in the PAD has been reported.

Comparing our results with those given in Refs. [4,6], the significant differences in the PADs suggest that in the corresponding regime the orbital angular momentum of the intermediate state cannot simply be assigned to the number of jets in the PAD. Even in the multiphoton regime, the empirical law based on dipole selection rule fails to describe the PAD due to the interference of different partial waves. Thus, for a specific resonant ionization process, the corresponding PAD may be altered significantly due to the interference between partial waves of the photoelectron.

IV. SUMMARY

In conclusion, resonant single ionization of the argon atom by linearly polarized laser field at relatively low intensities range from 1.1 to 4.55×10^{13} W/cm² is studied

employing the reaction microscope. At 4.55×10^{13} W/cm² intensity, the measured photoelectron energy spectra are in a good agreement with theoretical results of the time-dependent Schrödinger equation. Meanwhile, the $4p$ - $4d$ coupled resonant ionization peaks are clearly resolved in the spectra which confirms the theoretical predictions. However, the predicted positions of the peaks $4p$ and $4d$ are different from those of observed in our experiment. This discrepancy indicates that the single-active-electron model is not sufficient to describe resonant processes via low-lying states of $n = 4$.

As the intensity decreases below 2.0×10^{13} W/cm², the resonant ionization via $4f$ has been observed. However, although the TDSE calculation show that $l = 4$ is the dominant partial wave, the jetlike structure does not show any maximum at 90° either in the experimental or the theoretical results presented in this paper. Such a behavior implies destructive interference between different partial waves, namely, $l = 4$ and $l = 2$ and, hence, the empirical laws, wildly used in literature to assign the orbital angular momentum of the intermediate state to the number of jets in the PAD, might not apply even at the low intensity regime.

ACKNOWLEDGMENTS

B.N. gratefully acknowledges support from the National Natural Science Foundation of China (Grant No. 12164044) and the CAS President's Fellowship Initiative. X.Y. thanks Dr. M. Li from Huazhong University of Science and Technology for fruitful and constructive discussions.

-
- [1] P. Agostini and L. F. DiMauro, in *Advances in Atomic, Molecular, and Optical Physics*, edited by P. Berman, E. Arimondo, and C. Lin Advances In Atomic, Molecular, and Optical Physics Vol. 61 (Academic, San Dirgo, 2012), pp. 117–158.
 - [2] F. Krausz and M. Ivanov, *Rev. Mod. Phys.* **81**, 163 (2009).
 - [3] Y. Huismans, A. Rouzée, A. Gijsbertsen, P. S. W. M. Logman, F. Lépine, C. Cauchy, S. Zamith, A. S. Stodolna, J. H. Jungmann, J. M. Bakker, G. Berden, B. Redlich, A. F. G. van der Meer, K. J. Schafer, and M. J. J. Vrakking, *Phys. Rev. A* **87**, 033413 (2013).
 - [4] C. M. Maharjan, A. S. Alnaser, I. Litvinyuk, P. Ranitovic, and C. L. Cocke, *J. Phys. B: At., Mol. Opt. Phys.* **39**, 1955 (2006).
 - [5] G. D. Gillen and L. D. Van Woerkom, *Phys. Rev. A* **68**, 033401 (2003).
 - [6] T. Marchenko, H. G. Muller, K. J. Schafer, and M. J. J. Vrakking, *J. Phys. B: At., Mol. Opt. Phys.* **43**, 095601 (2010).
 - [7] R. Wiehle, B. Witzel, V. Schyja, H. Helm, and E. Cormier, *J. Mod. Opt.* **50**, 451 (2003).
 - [8] P. Kaminski, R. Wiehle, V. Renard, A. Kazmierczak, B. Lavorel, O. Faucher, and B. Witzel, *Phys. Rev. A* **70**, 053413 (2004).
 - [9] M. Schuricke, G. Zhu, J. Steinmann, K. Simeonidis, I. Ivanov, A. Kheifets, A. N. Grum-Grzhimailo, K. Bartschat, A. Dorn, and J. Ullrich, *Phys. Rev. A* **83**, 023413 (2011).
 - [10] M. Li, Y. Liu, H. Liu, Y. Yang, J. Yuan, X. Liu, Y. Deng, C. Wu, and Q. Gong, *Phys. Rev. A* **85**, 013414 (2012).
 - [11] M. Li, P. Zhang, S. Luo, Y. Zhou, Q. Zhang, P. Lan, and P. Lu, *Phys. Rev. A* **92**, 063404 (2015).
 - [12] A. Rudenko, K. Zrost, C. D. Schröter, V. L. B. de Jesus, B. Feuerstein, R. Moshhammer, and J. Ullrich, *J. Phys. B: At., Mol. Opt. Phys.* **37**, L407 (2004).
 - [13] D. G. Arbó, S. Yoshida, E. Persson, K. I. Dimitriou, and J. Burgdörfer, *Phys. Rev. Lett.* **96**, 143003 (2006).
 - [14] M. Wickenhauser, X. M. Tong, D. G. Arbó, J. Burgdörfer, and C. D. Lin, *Phys. Rev. A* **74**, 041402(R) (2006).
 - [15] J. Wiese, J.-F. Olivieri, A. Trabattoni, S. Trippel, and J. Küpper, *New J. Phys.* **21**, 083011 (2019).
 - [16] J. Zhang, W. Zhang, Z. Xu, X. Li, P. Fu, D.-S. Guo, and R. R. Freeman, *J. Phys. B: At., Mol. Opt. Phys.* **35**, 4809 (2002).
 - [17] H. R. Reiss, *Phys. Rev. A* **22**, 1786 (1980).
 - [18] L. Bai, J. Zhang, Z. Xu, and D.-S. Guo, *Phys. Rev. Lett.* **97**, 193002 (2006).
 - [19] Z. Chen, T. Morishita, A.-T. Le, M. Wickenhauser, X. M. Tong, and C. D. Lin, *Phys. Rev. A* **74**, 053405 (2006).
 - [20] D. G. Arbó, K. I. Dimitriou, E. Persson, and J. Burgdörfer, *Phys. Rev. A* **78**, 013406 (2008).
 - [21] R. R. Freeman, P. H. Bucksbaum, H. Milchberg, S. Darack, D. Schumacher, and M. E. Geusic, *Phys. Rev. Lett.* **59**, 1092 (1987).
 - [22] P. H. Bucksbaum, R. R. Freeman, M. Bashkansky, and T. J. McIlrath, *J. Opt. Soc. Am. B* **4**, 760 (1987).
 - [23] V. Schyja, T. Lang, and H. Helm, *Phys. Rev. A* **57**, 3692 (1998).
 - [24] M. Schuricke, K. Bartschat, A. N. Grum-Grzhimailo, G. Zhu, J. Steinmann, R. Moshhammer, J. Ullrich, and A. Dorn, *Phys. Rev. A* **88**, 023427 (2013).

- [25] M. Krug, T. Bayer, M. Wollenhaupt, C. Sarpe-Tudoran, T. Baumert, S. Ivanov, and N. Vitanov, *New J. Phys.* **11**, 105051 (2009).
- [26] P. Ge, M. Han, M.-M. Liu, Q. Gong, and Y. Liu, *Phys. Rev. A* **98**, 013409 (2018).
- [27] X. Gong, C. Lin, F. He, Q. Song, K. Lin, Q. Ji, W. Zhang, J. Ma, P. Lu, Y. Liu, H. Zeng, W. Yang, and J. Wu, *Phys. Rev. Lett.* **118**, 143203 (2017).
- [28] R. Wiehle, B. Witzel, H. Helm, and E. Cormier, *Phys. Rev. A* **67**, 063405 (2003).
- [29] B. Hai, S. F. Zhang, M. Zhang, B. Najjari, D. P. Dong, J. T. Lei, D. M. Zhao, and X. Ma, *Phys. Rev. A* **101**, 052706 (2020).
- [30] M. Zhang, B. Najjari, B. Hai, D.-M. Zhao, J.-T. Lei, D.-P. Dong, S.-F. Zhang, and X.-W. Ma, *Chin. Phys. B* **29**, 063302 (2020).
- [31] Y. Shao, M. Li, M.-M. Liu, X. Sun, X. Xie, P. Wang, Y. Deng, C. Wu, Q. Gong, and Y. Liu, *Phys. Rev. A* **92**, 013415 (2015).
- [32] J. Ullrich, R. Moshhammer, A. Dorn, R. Dörner, L. P. H. Schmidt, and H. S.-B. cking, *Rep. Prog. Phys.* **66**, 1463 (2003).
- [33] M. Li, J.-W. Geng, H. Liu, Y. Deng, C. Wu, L.-Y. Peng, Q. Gong, and Y. Liu, *Phys. Rev. Lett.* **112**, 113002 (2014).
- [34] T. Morishita, Z. Chen, S. Watanabe, and C. D. Lin, *Phys. Rev. A* **75**, 023407 (2007).
- [35] H. G. Muller and F. C. Kooiman, *Phys. Rev. Lett.* **81**, 1207 (1998).
- [36] S. H. Autler and C. H. Townes, *Phys. Rev.* **100**, 703 (1955).
- [37] X. Wu, Z. Yang, S. Zhang, X. Ma, J. Liu, and D. Ye, *Phys. Rev. A* **103**, L061102 (2021).
- [38] H. Helm, N. Bjerre, M. J. Dyer, D. L. Huestis, and M. Saeed, *Phys. Rev. Lett.* **70**, 3221 (1993).

Correction: A funding source in the Acknowledgments contained an error and has been fixed.